CrossMark

ORIGINAL PAPER

An in-depth study on crystallization kinetics of PET/PLA blends

Hasan Azizi Topkanlo[1] · Zahed Ahmadi[2] · Faramarz Afshar Taromi[1,2]

Abstract The crystallization behavior and mechanical properties of PET/PLA blends with various amounts of PLA were investigated using a wide angle X-ray diffraction (WAXD), differential scanning calorimeter (DSC) and tensile analyses. The crystallization rate and relative crystallinity of the PET/PLA blends were studied by theoretical models of Kissinger, Avrami, Ziabicki and Ozawa. The WAXD analysis showed that the PLA phase was wholly amorphous in all blends after cooling from the melt to ambient temperature. Crystallization behavior assessments on PET/PLA blends suggest that PLA acts as a nucleating agent for PET phase leading to an increase in the initial and peak crystallization temperatures. Kissinger's model showed a rise in activation energy up to 72% for the PET/PLA blends containing 30 wt% PLA. Ziabicki's model gave a minimum value for kinetic parameter in PET/PLA (70/30 w/w) due to the nucleating action of PLA. On the other hand, PLA acted as a retarder for chain segments of PET tending to diffuse through the surface of growing crystals. Therefore, at an optimal composition of PET/PLA, crystallization occurs appropriately. However, an increase in PET content leads to fall in ductility, tensile strength, modulus, elongation-at-break, and fracture toughness of PET/PLA blends.

Introduction

Poly(lactic acid) (PLA) is a biodegradable thermoplastic aliphatic polyester [1] which is used for manufacturing consumer products [2] , biodegradable medical devices [3] and 3D-printed prototypes [4]. In recent years, PLA is developed as one of the highest recognized compostable thermoplastics to replace the traditional synthetic polymers for controlling the environmental pollutions [5–7]. However, PLA has a low oxygen barrier property with low thermal stability which is not appropriate for industrial operations [8, 9].

Blending is one of the most used and low-cost methods to improve the properties of polymers for development and commercialization of new materials [10]. Several blends of PLA with other polymers have been employed to improve the mechanical properties [11, 12], degradation behavior [13], processability [14] and crystallization [15]. Diaz et al. [16] have reported the effect of several polymers on the film performance of PLA binary blends and found that the blending of PLA with polycaprolactone (PCL), polybutylene succinate and ethylene vinyl acetate leads to the improvement of tear resistance. Ferri et al. [17] have studied the mechanical properties of PLA/PCL blends and found that the PCL has a marked effect on the ductile properties. However, the slight increase in melt temperature of PLA indicates the low miscibility of PLA and PCL. Pattamaprom et al. [18] investigated the effect of natural rubber (NR) on the impact strength of PLA and reported that the highest impact strength could be achieved by NR when masticated at 40 rpm for 15 min. Semba et al. [19] prepared the PLA/PCL blends cured with dicumyl peroxide and found that the

✉ Zahed Ahmadi
  zahmadi@aut.ac.ir

[1] Department of Polymer Engineering and Color Technology, Amirkabir University of Technology, Tehran, Iran

[2] Department of Chemistry, Amirkabir University of Technology, Tehran, Iran

IPPI Springer

ultimate tensile strength was significantly improved which the resulted mechanical properties were comparable to those of high impact polystyrene.

Polyethylene terephthalate (PET) is one of the most used polymers in packaging industries with low permeability and good mechanical properties [20–22]. Therefore, PET is a good candidate for blending with PLA to achieve a biodegradable material for packaging and bottle manufacturing with appropriate barrier properties. Xia et al. [23] have focused on lowering the degradation temperature of PET/PLA blends and found that the PLA concentration has a considerable effect on lowering thermal stability and mechanical properties. Chen et al. [24] have investigated the non-isothermal crystallization of PET/PLA blends and reported that PLA can crystallize in both amorphous and crystalline PLA. However, the degree of PET crystallinity decreases with PLA loading. Huerta et al. [25] studied the miscibility in PET/PLA blend and compared the state of compatibility with PET/chitosan blends. They found that the miscibility of PLA is higher than chitosan and the saturation of PLA into the polymer matrix could be reached to 10 wt% level.

The present study explores the mechanical properties and non-isothermal crystallization behavior of PLA/PET blends from the melt for a wide range of PLA/PET ratios. The PLA/PET blends were prepared through a melt-mixing procedure. Several characterization techniques including differential scanning calorimeter (DSC) with various heating rates, wide angle X-ray diffraction (WAXD) and tensile measurements were employed to investigate the crystalline structure and mechanical behavior of PLA/PET blends. The non-isothermal crystallization behavior of the prepared blends was analyzed through several theoretical models and compared with experimental results.

Experimental

Materials

Poly(lactic acid) (PLA) was purchased from Nature Works LLC, USA, containing 1.5–2% of D isomer (PLA-2002D grade) with onset degradation of 290 °C, molecular weight of 2.71×10^5 g/mol and MFI of 12.4 g/10 min. PET bottle grade chips (BG-821) with intrinsic viscosity of 0.82 dL/g and melting point of 248 °C was provided by Shahid Tond-guyan Petrochemical Co., Iran.

Preparation

PLA and PET were dried at 60 °C for 24 h in a vacuum oven before blends preparation. The blends with various PLA/PET ratios including 100, 90, 70 and 50 were prepared through a direct melt-mixing process in a laboratory size internal mixer (Brabender Plasti-Corder, W50, Germany) at 260 °C and 60 rpm for 6 min. The neat PLA and PET were also separately compounded as reference materials for comparison purposes. The prepared samples were compression molded by hot press at 260 °C for 5 min to obtain suitable samples for tensile measurements.

Characterization

Wide angle X-ray analysis (WAXD) was carried out using X-ray diffractometer (Philips PANalytical X'pert PRO) with Cu Kα radiation ($\lambda = 1.540598$ Å) at a generator voltage of 40 kV and 40 mA current at room temperature. Bragg's law, $n\lambda = 2d \sin\theta$, was used to compute the crystallographic spacing (d) of the samples. The range of 2θ scanning of X-ray intensity employed was 1°–45° with a scanning rate of 1° min^{-1}.

Crystallization and melting temperatures of the prepared samples was performed using a Setaram 131 (France) differential scanning calorimeter (DSC) under a nitrogen atmosphere. Cold crystallization behavior of PLA/PET blends was investigated through heating up to 280 °C where the heating rate was 5 °C/min. Then, the samples were remained at this temperature for 5 min to eliminate thermal history. Next, the PLA/PET blends were cooled down to ambient temperature with cooling rate of 20 °C/min. The crystallinity of each phase was calculated through the following equation [26]:

$$X_c = \frac{\Delta H_c}{w \times \Delta H_0} \times 100, \tag{1}$$

where X_c is the percent of crystal phase, ΔH_c is the melting enthalpy of crystallization of PET or PLA in the blend, w is the weight fraction of each phase in the blend and ΔH_0 is the melting enthalpy of 140 J/g [27] for 100% crystalline PET and 93 J/g for 100% crystalline PLA [28].

Non-isothermal crystallization was investigated through heating of the samples up to 280 °C with heating rate of 80 °C/min. The samples were remained at the mentioned temperature for 5 min to eliminate the thermal history. After that, the PLA/PET blends were cooled down to ambient temperature with various cooling rates including 5, 10 and 15 °C/min. The required time to reach 50% of complete crystallization of PET phase in the blends could be calculated for various cooling rates using the following equation [29]:

$$t_{1/2} = \frac{T_0 - T}{R}, \tag{2}$$

where R is the cooling rate, T_0 and T are the temperatures at start point and 50% of crystallization process, respectively. Isothermal crystallization behavior of PLA/PET blends were explored through heating up to 280 °C with heating rate of 80 °C/min and remaining at this temperature for 5 min.

Then, the samples were cooled down to 200 °C with cooling rate of 20 °C until the crystallization was completely performed.

Tensile properties of the PLA/PET blends were explored at a cross–head speed of 1 mm/min using a DBBP-5t universal testing machine according to ASTM D882-09. The samples were prepared in a rectangular form with dimensions of 10 × 2 cm.

Results and discussion

Wide angle X-ray scattering

The XRD patterns of PLA/PET blends are shown in Fig. 1 and compared to owners of pristine PLA and PET. Miller indices [30] are marked above the XRD patterns of pristine polymers. PLA Miller indices refer to alpha phase which indicated the orthorhombic crystal structure [30]. The other peaks in XRD pattern of PLA are related to the stereo complex crystals (sc) which is indicated in Fig. 1. However, the crystal peaks in PLA/PET blends are related to the PET crystals. It should be noted that the crystallization temperature of PLA is lower than PET. Therefore, the PET crystallizes from the melt in the presence of fully molten PLA. The results show that the PLA phase is still wholly amorphous in all the blends after cooling from the melt to ambient temperature.
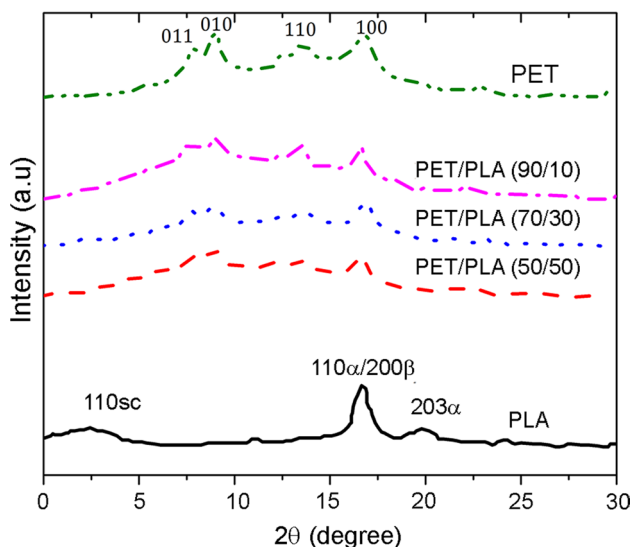
Cold crystallization behavior

Figure 2 reveals the cold crystallization behaviors of PLA, PET and the blends of PLA/PET containing various PET loadings. As can be seen from this figure, the PLA phase has been crystallized at lower temperatures compared to the PET component during the heating process. However, introduction of PET into PLA leads to a drop in cold crystallization of PLA especially at higher PLA concentrations. Table 1 shows the various calculated parameters from cold crystallization measurements. Table 1 indicates that the peak cold crystallization temperature of PLA is dependent on the percent of crystallized PET phase in the PLA/PET blends. So that the PLA phase is crystallized at lower temperatures with higher weight percentage of crystallized PET component.

Non-isothermal crystallization

The effect of PLA on non-isothermal crystallization behavior of PET component in PLA/PET was studied by DSC with various cooling rates. A non-isothermal crystallization behavior of PLA/PET blends at a cooling rate of 10 °C/min is depicted in Fig. 3. Crystallization temperature of PET increased with PLA concentration due to the nucleating effect of PLA phase [31]. Table 2 shows the non-isothermal crystallization data for PLA/PET blends containing various PET concentrations. As depicted in this table, the initial and peak crystallization temperatures are decreased with increases in cooling rate from 5 to 15 °C/min.

It seems that at lower cooling rates, the polymer chains have enough time to overcome the nucleation obstacles [32]. Therefore, the initial crystallization temperatures may shift to higher contents. However, the crystallization temperature
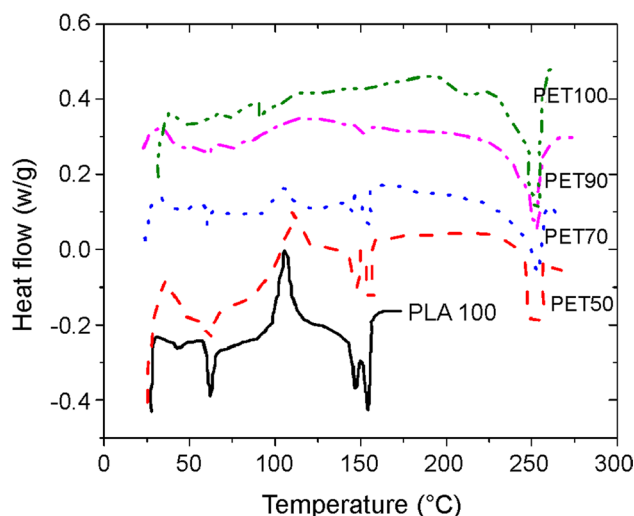

Fig. 1 XRD patterns of neat PLA, neat PET and PET/PLA blends with different compositions

Fig. 2 Cold crystallization behavior of neat PLA, neat PET and PET/PLA blends with different PET weight percentages

Table 1 Cold crystallization data of PET and PLA parent polymers and their blends having different compositions

PET/PLA ratio→	100/0		90/10		70/30		50/50		0/100	
Properties	PET	PLA	PET	PLA	PET	PLA	PET	PLA	PET	PLA
T_c (°C)	–	–	–	–	–	103.9	–	111.3	–	106.3
T_{m1} (°C)	–	–	–	–	–	146	–	148.1	–	147.6
T_{m2} (°C)	–	–	–	–	–	154.8	–	156.1	–	155
T_{mPET} (°C)	253.9	–	253.4	–	252.7	–	252.2	–	–	–
H_{cc} (J/g)Δ	–	–	–	–	–	9.1	–	16.5	–	22.8
H_m (J/g)Δ	52.5	–	41	–	17.2	10	13.2	17.2	–	25.4
X_c (%)	37.5	–	32.5	–	17.5	3.2	18.8	1.5	–	2.7
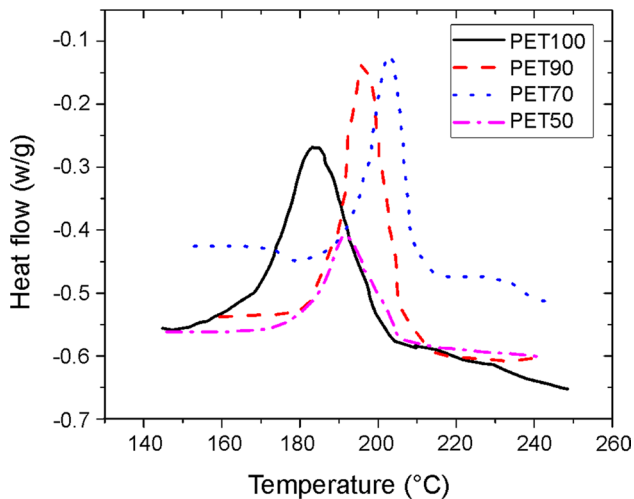
Fig. 3 Non-isothermal crystallization behavior of neat PET and PET/PLA blends having different contents of PET under 10 °C/min cooling rate

range is dropped with increase in cooling rate. Table 2 shows that an increase in cooling rate leads to higher crystallization temperature range with lower weight percentage of crystals due to some possible defects in crystal structure of PET component [33].

Kissinger [34] has proposed a method to calculate the activation energy needed for diffusion of polymer segments into the surface of growing crystals as follows:

$$\frac{d\left(\ln \frac{x}{T_p^2}\right)}{d\left(\frac{1}{T_p}\right)} = -\Delta E/R \qquad (3)$$

where T_p is peak crystallization temperature, x is cooling rate, ΔE is activation energy and R is universal gas constant.

Figure 4 demonstrates the Kissinger's diagram for PLA/PET blends containing various PET loadings. The calculated activation energy (Table 3) for diffusion of PET segments into the surface of growing crystals is increased with higher PLA loadings due to the reduced chain mobility of PET component. It should be noted that the activation energy has been increased up to 72% for PLA/PET blends containing 30 wt% of PLA phase.

Figure 5 displays the Jabarin's method [35] for determination of minimum required cooling rate to achieve a fully amorphous PLA/PET blend on the basis of weight percentage extrapolation of crystal phase to zero content with respect to the cooling rate. Table 3 displays the calculated cooling rates to achieve a fully amorphous blend which is

Table 2 Non-isothermal crystallization data for PET and PLA parent polymers and their blends having different compositions

|	Cooling rate (°C/min)											
PET/PLA ratio→	100/0			90/10			70/30			50/50		
Properties↓	5	10	15	5	10	15	5	10	15	5	10	15
T_{onset} (°C)	205.4	201	195.2	210.7	206	201.2	213.4	208.4	207.3	210.5	203.2	197.7
T_{endset} (°C)	175.7	161.1	150.1	188.6	182.6	175.4	196.7	187.9	185.6	194.5	178.8	170.7
$T_{onset} - T_{endset}$	29.7	39.1	45.1	15.4	23.4	28.8	17.3	20.5	21.7	16	24.4	27.7
T_p (°C)	197.1	185.4	180.7	203.3	197.1	191.4	207.3	203.1	198.9	203.2	192.6	186.5
$T_{onset} - T_p$	14.3	14.7	14.5	7.2	8.9	9.8	6.1	5.3	8.4	7.5	10.6	11.2
H_c (J/g)Δ	38.2	35.7	35.0	30.5	28.5	27.1	20.2	18.1	16.4	15.3	14.2	12.9
X_c (%)	45.2	42.3	41.5	40.1	37.4	35.6	34.8	31.1	27.6	36.2	33.6	30.7
$t_{1/2}$ (s)	183	99	77	93	57	43	92	42	35	95	70	49
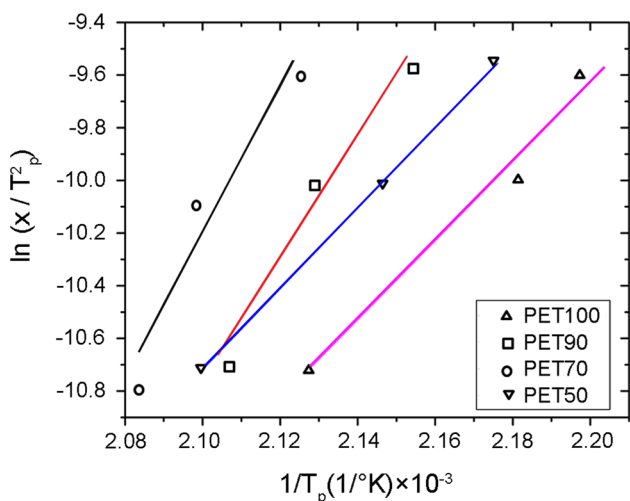
Fig. 4 Kissinger plots for neat PET and PET/PLA blends having different contents of PET

Table 3 The obtained parameters from Kissinger's and Jabarin's methods for a neat PET and its blends with PET having different compositions

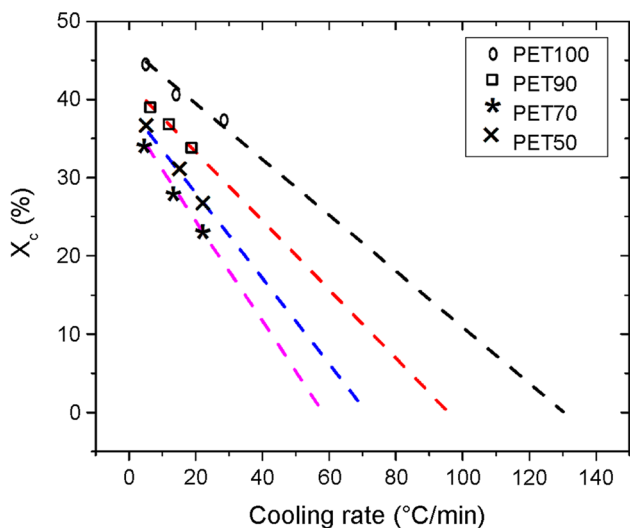| PET/PLA ratio	Activation energy (kJ/mol)	Cooling rate (°C/min)
100/0	124.43	130.60
90/10	178.95	95.96
70/30	228.25	58.10
50/50	127.00	71.64

Fig. 5 Effect of cooling rate on the crystallinity of neat PET and PET/PLA blends having different contents of PET
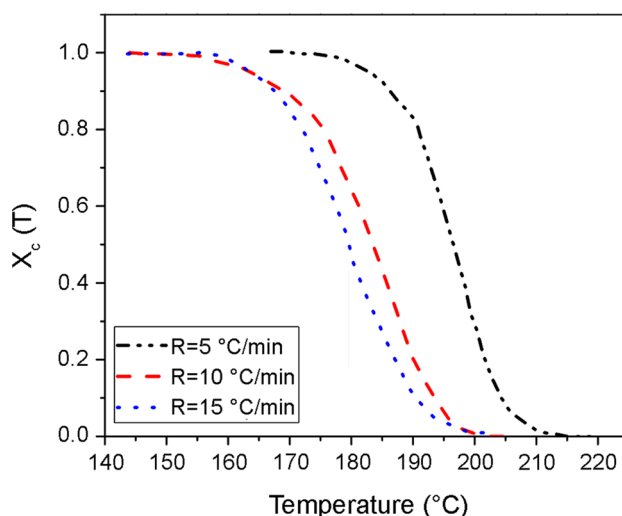

Fig. 6 Relative crystallinity calculated for a neat PET

decreased with PLA phase concentration. These results may suggest that PLA can reduce the crystallinity of PET component. It can be concluded that the processing parameters such as the cooling rate has a considerable effect on crystal morphology of PLA/PET blends which could lead to a fully amorphous blends with desired properties.

Relative crystallinity of PLA/PET blends with respect to temperature is defined by the following equation [36]:

$$X_C(T) = \frac{\int_{T_0}^{T} \left(\frac{dH}{dT} \right) dT}{\int_{T_0}^{T_\infty} \left(\frac{dH}{dT} \right) dT}, \tag{4}$$

where $X_C(T)$ is the relative crystallinity, T_0 and T_∞ are initial and final crystallization temperatures, respectively.

The effect of cooling rate on the degree of crystallinity of neat PET can be studied using Fig. 6 (Fig. S1 shows such plots for blends containing various amounts of PET).

According to the figures, as the cooling rate is increased the relative crystallinity is decreased for a specific temperature due to less chances for polymer chains to overcome the nucleating obstacles. The relative crystallinity has a tendency to approach 100% at higher temperatures as the cooling rate is decreased. It means that the crystal structures of PET/PLA blends need to be completed at higher temperatures as the cooling rate is decreased. The time required to reach 50% PET crystallization completion calculated for the studied systems (Table 2) suggests that addition of PLA to the PET phase increases the crystallization rate of PET component.

Ziabicki [37] assumed that the crystallization rate $((dX_c(T)/dT)_R)$ with respect to temperature would follow by Gaussian function at constant cooling rate. He proposed a

model for kinetic parameter (G) of crystallization on the basis of the above hypothesis:

$$G = \int_{T_g}^{T_m} K(T)\mathrm{d}(T) \approx 1.064 K_{max} D_R = 1.064 \left(\frac{\mathrm{d}X_C(T)}{\mathrm{d}T} \right)_{R,max} D_R,$$
(5)

where T_g and T_m are glass transition and melting temperatures, respectively. $K(T)$ is the function of crystallization rate and K_{max} is the maximum crystallization rate or the peak height of the crystallization rate curve with respect to temperature. D_R is defined as the width of the peak curve multiplied by half of the peak height of crystallization rate curve. Table 4 reveals the maximum crystallization rate and corresponding temperature, kinetic parameter of crystallization and the average kinetic parameter.

A comparison between Tables 2 and 4 shows that T_R in Table 4 is about equal to T_p. As can be seen from Table 4, the crystallization rate increases with cooling rate for each sample. Table 4 shows that the kinetic parameter of crystallization decreases with PLA loadings which may imply less ability in crystallization. However, there is a minimum value for kinetic parameter in PET/PLA (70/30 w/w). It seems that PLA can act as a nucleating agent as it increases the crystallization temperature, while it can act as a retarder for PET chain segments to diffuse in the surface of growing crystals. Therefore, the PLA/PET blends must have an optimum ratio in view of crystallization behavior.

Ozawa [38] proposed a model for prediction of relative crystallization with respect to temperature as the following equation:

$$x_c(T) = 1 - \exp(K(T)/R)^n$$
(6)

where $x_c(T)$ is relative crystallization at temperature of T, $K(T)$ is a function of crystallization rate, R is cooling rate and n is Ozawa's index.

Equation 6 can be re-written as the following logarithmic form:

$$\log[-\ln(1 - x_c(T))] = n \log(K(T)) - n \log(R)$$
(7)

$K(T)$ and n can be calculated from intercept and slope of the left side line of Eq. 7 with respect to log(R). Typical such plots, obtained at different temperatures, are provided in Fig. 7 for a neat PET. Plots of different blend compositions are available in Fig. S2.

Figure S3 shows variation of $K(T)$ and n as a function of temperature for the neat PET and its blends with PLA having different compositions, as summarized in Table 5. The temperatures referred in this table for each sample comprise the temperature range which the relative crystallization could be a function of Ozawa's equation. It can be understood from the trend in n and $K(T)$ that as the temperature lowers, the Ozawa index n decreases, while $K(T)$ follows an increasing order which implies feasibility in crystallization at low temperatures. The blend containing 30 wt% PLA takes the minimum value of n, though the maximum value of $K(T)$ suggests high activation energy of chain segments to diffuse into the surface of the growing crystals [39]. Such observations are in full agreement with the trends observed in Table 2.
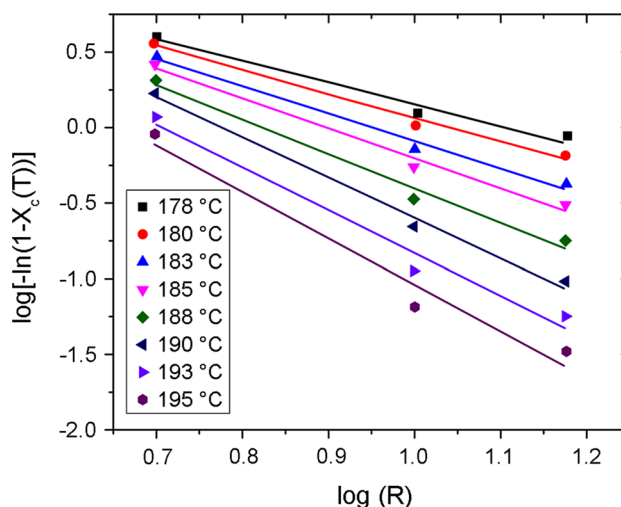

Fig. 7 Typical of Ozawa plots obtained at constant temperature for a neat PET

Table 4 The results of Ziabicki's model for a neat PET and its blends with PET having different compositions

PET/PLA ratio→	Cooling rate (°C/min)											
	100/0			90/10			70/30			50/50		
Properties ↓	5	10	15	5	10	15	5	10	15	5	10	15
$T_{R,max}$ (°C)	197.2	185.3	180.6	203.3	197.2	191.4	207.2	203.1	198.9	203.3	192.6	185.5
$(\mathrm{d}X_c(T)/\mathrm{d}T)_{R,max}$ (1/min)	0.325	0.485	0.70	0.455	0.865	1.078	0.483	1.030	1.457	0.445	0.712	0.900
D_R (°C)	14.1	19.0	21.3	10.10	10.7	12.93	8.30	5.8	9.4	10.1	12.5	14.0
G_R	0.92	0.92	1.00	0.90	0.91	0.92	0.80	0.85	0.91	0.90	0.89	0.84
$G_{R-average}$	0.95			0.90			0.85			0.88		

Table 5 K (T) and n for a neat PET and its blends with PET having different compositions

PET/PLA ratio	T (°C)	n	K (°C/min)
100/0	178	1.43	12.8
	180	1.57	10.96
	183	1.80	8.92
	185	1.98	7.89
	188	2.27	6.64
	190	2.65	5.97
	193	2.82	5.09
	195	3.08	4.60
90/10	185	0.91	28.3
	188	1.01	17.71
	190	1.06	16.20
	193	1.50	10.99
	195	1.89	9.05
	197	2.12	7.54
	200	2.40	6.42
70/30	190	0.91	34.48
	192	0.92	30.30
	193	0.93	26.31
	195	1.05	16.84
	197	1.27	11.48
50/50	192	3.64	8.91
	194	3.68	8.20
	195	4.04	7.20
	197	4.64	6.49

Fig. 8 Crystallization behavior of a neat PET and PET/PLA blends having different contents of PET at 200 °C

where $\frac{dH}{dt}$ is the rate of evolved heat.

Figure 9 represents the relative isothermal crystallization of PET phase in various PLA/PET blends at temperature of 200 °C. It is obvious that the PLA can increase the overall crystallization rate of PET phase due to the nucleating effects especially at 30 wt% of PLA loading.

The coefficients of isothermal crystallization kinetic for various PLA/PET blends were determined through Avrami's theory [42] as the following equation:

$$X_t = 1 - \exp(-Kt^n) \tag{9}$$

where n is the Avrami's power and k is the crystallization rate constant. Equation 9 can be represented in logarithmic form as follows:

$$\log[-\ln(1 - X_t)] = \log(K) + n\log(t) \tag{10}$$

Figure 10 shows the plot of $\log[-\ln(1 - X_t)]$ with respect to $\log(t)$ for a neat PET polymer at temperature of 200 °C. Moreover, Fig. S4 shows such plots for the blend samples. The parameters of n and K for each sample were calculated from the slope and intercept of the straight lines passed through the experimental data. The results indicated that the Avrami's power roughly remains unchanged with PLA

Isothermal crystallization

The isothermal crystallization behavior of PET phase in various PLA/PET blends at temperature of 200 °C is depicted in Fig. 8. The resulting parameters of isothermal crystallization measurements of PLA/PET blends are presented in Table 6.

The parameter Δt reveals the required time to reach the crystallization peak or required time to complete the crystallization process [40]. As it is evident in Fig. 8 and Table 6, the required time for crystallization of PET phase decreases with PLA content in reaching 30 wt% due to the nucleating effect of PLA component in the PLA/PET blends. It can be concluded that the PLA phase can increase the rate of crystallization of PET phase with its maximum rate by a PLA/PET blend of 30/70 w/w.

The relative crystallization (X_t) of PET phase in isothermal crystallization measurements could be determined using the following equation [41]:

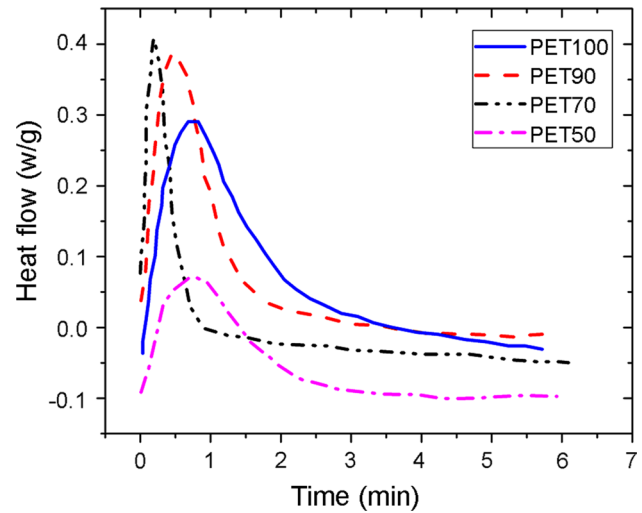$$X_t = \frac{\int_0^t \frac{dH}{dt} dt}{\int_0^\infty \frac{dH}{dt} dt}. \tag{8}$$

Table 6 Isothermal crystallization parameters for a neat PET and its blends with PET having different compositions

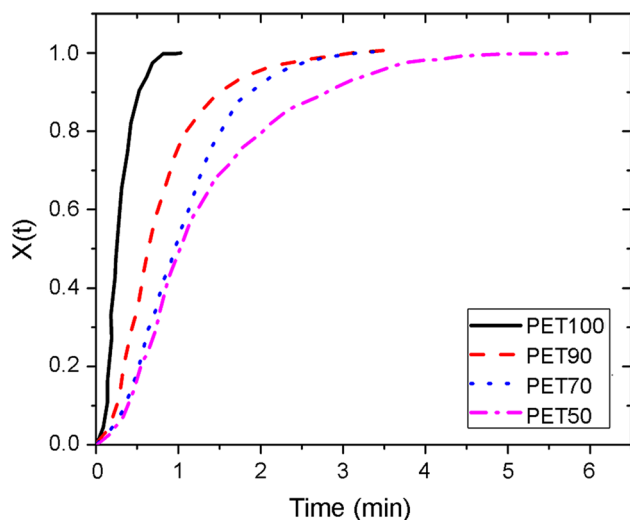| PET/PLA ratio	Δt (s)	X_c (%)	ΔH_c (J/g)	$t_{1/2}$ (s)
100/0	57	37.8	31.9	65
90/10	34	30.5	23.1	40
70/30	14	16.6	9.9	17
50/50	50	29.7	12.6	58

Fig. 9 Relative isothermal crystallization with respect to crystallization time for neat PET and PET/PLA blends having different contents of PET

Fig. 11 Stress–strain curves for neat PET and PET/PLA blends having different contents of PET

Table 7 Mechanical properties for a neat PET and its blends with PET having different compositions

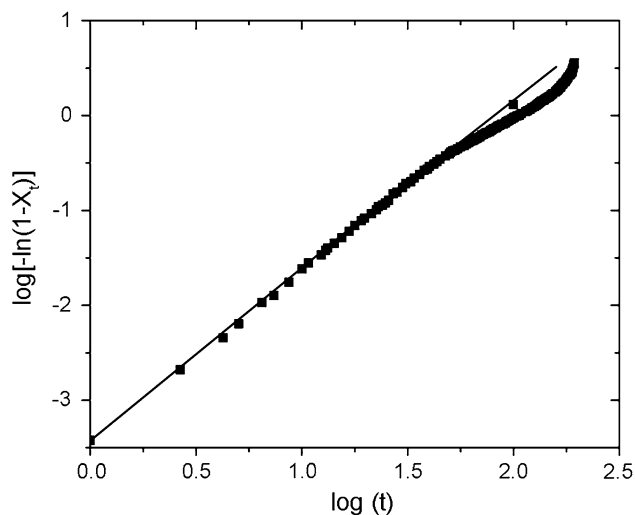| PET/PLA ratio	Yield strength (MPa)	Tensile strength (MPa)	Yield strain (%)	Strain-at-break (%)	Young's modulus (MPa)
90/10	40	46	2.7	7.8	1481
70/30	–	36	–	4.2	857
50/50	–	27	–	3.3	818
0/100	–	22	–	3.09	711

Fig. 10 Avrami plot at temperature of 200 °C for neat PET

loadings. It seems that the crystallinity of PET phase at the growing stage is independent of PLA concentrations which leads to a two dimensional growth of PET crystals in a plane.

Mechanical properties

Mechanical properties of blends containing various PLA contents are shown in Fig. 11 and the related parameters are given in Table 7. It is clear that an increase in PET concentration leads to deterioration of ductility and tensile strength of the blends. Table 7 shows that an increase in PET loadings causes a decrease in Young's modulus and elongation-at-break of the prepared blends. The results suggest that
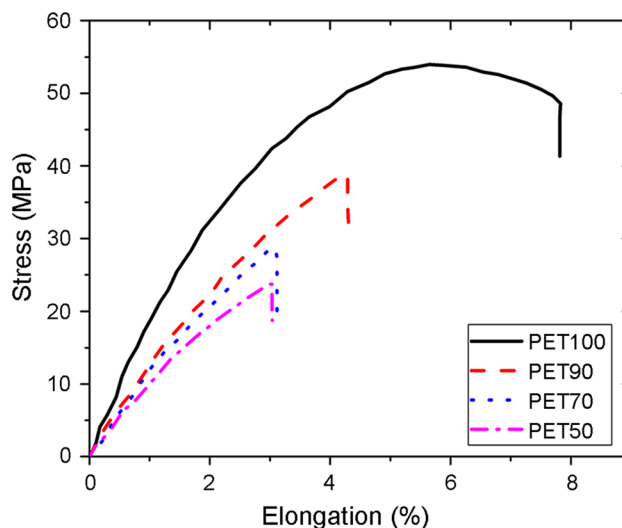
introduction of PET into the blends leads to a brittle behavior in view of fracture toughness.

Conclusion

The PLA/PET blends were prepared through a melt-mixing procedure for packaging applications. The crystallization behavior and mechanical properties of PLA/PET blends containing various PLA loadings were explored through WAXD, DSC and tensile tests measurements. The results of WAXD analysis showed that the PLA phase was still wholly amorphous in all blends after cooling from the melt to ambient temperature. The results of cold crystallization analysis showed that the peak cold crystallization temperature of PLA is dependent on the percentage of crystallized PET phase in the PLA/PET blends. Non-isothermal crystallization measurements show that the crystallization temperature of PET is increased with PLA concentration due to the nucleating effect of PLA phase. The results indicate that the initial and peak crystallization temperatures are decreased with increases in cooling rate. However, the crystallization

temperature range is decreased with increases in cooling rate. The calculated activation energy, using Kissinger's equation for diffusion of PET segments into the surface of growing crystals, is increased with higher PLA loadings. It can be concluded that the relative crystallinity has a tendency to unity at higher temperatures as the cooling rate is decreased. The applicability of Ozawa's equation for non-isothermal crystallization behavior of PLA/PET has been studied and the results show that the ability of crystallization is increased when temperature is decreased. The PLA/PET blends containing 30 wt% of PLA display the minimum value of Ozawa's index and maximum value of $K(T)$ which indicate a high activation energy of polymer segments to diffuse into the surface of growing crystals. The active parameters of isothermal crystallization measurements of PLA/PET blends have revealed that the required time for crystallization of PET phase decreases with PLA content up to 30 wt%. In this respect, the PLA phase can increase the rate of crystallization of PET phase which has a maximum rate in PLA/PET (30/70 w/w) blends. Mechanical properties of PLA/PET blends containing various PLA loadings indicated that an increase in PET concentration leads to lower ductility and tensile strength of PLA/PET blends. It can be concluded that an increase in PET loadings leads to lower Young's modulus and elongation-at-break of the prepared blends. The results suggest that introducing PET into the blends leads to a brittle behavior in view of fracture toughness.

References

1. Garlotta D (2001) A literature review of poly(lactic acid). J Polym Environ 9:63–84
2. Datta R, Henry M (2006) Lactic acid: recent advances in products, processes and technologies—a review. J Chem Technol Biotechnol 81:1119–1129
3. Tyler B, Gullotti D, Mangraviti A, Utsuki T, Brem H (2016) Polylactic acid (PLA) controlled delivery carriers for biomedical applications. Adv Drug Deliv Rev 107:163–175
4. Tymrak B, Kreiger M, Pearce JM (2014) Mechanical properties of components fabricated with open-source 3-D printers under realistic environmental conditions. Mater Design 58:242–246
5. Nampoothiri KM, Nair NR, John RP (2010) An overview of the recent developments in polylactide (PLA) research. Bioresour Technol 101:8493–8501
6. Fukushima K, Abbate C, Tabuani D, Gennari M, Camino G (2009) Biodegradation of poly(lactic acid) and its nanocomposites. Polym Degrad Stabil 94:1646–1655
7. Li M-X, Kim S-H, Choi S-W, Goda K, Lee W-I (2016) Effect of reinforcing particles on hydrolytic degradation behavior of poly(lactic acid) composites. Compos Part B: Eng 96:248–254
8. Drieskens M, Peeters R, Mullens J, Franco D, Lemstra PJ, Hristova-Bogaerds DG (2009) Structure versus properties relationship of poly(lactic acid). I. Effect of crystallinity on barrier properties. J Polym Sci Part B Polym Phys 47:2247–2258
9. Yao L, Wang Y, Li Y, Duan J (2017) Thermal properties and crystallization behaviors of polylactide/redwood flour or bamboo fiber composites. Iran Polym J 26:161–168
10. Yu L, Dean K, Li L (2006) Polymer blends and composites from renewable resources. Prog Polym Sci 31:576–602
11. Suyatma NE, Copinet A, Tighzert L, Coma V (2004) Mechanical and barrier properties of biodegradable films made from chitosan and poly(lactic acid) blends. J Polym Environ 12:1–6
12. Deetuam C, Samthong C, Pratumpol P, Somwangthanaroj A (2017) Improvements in morphology, mechanical and thermal properties of films produced by reactive blending of poly(lactic acid)/natural rubber latex with dicumyl peroxide. Iran Polym J 26:615–628
13. Dai X, Cao Y, Shi X, Wang X (2016) Non-isothermal crystallization kinetics, thermal degradation behavior and mechanical properties of poly(lactic acid)/MOF composites prepared by melt-blending methods. RSC Adv 6:71461–71471
14. As' habi L, Jafari SH, Khonakdar HA, Boldt R, Wagenknecht U, Heinrich G (2013) Tuning the processability, morphology and biodegradability of clay incorporated PLA/LLDPE blends via selective localization of nanoclay induced by melt mixing sequence. Express Polym Lett 7:21–39
15. Li FJ, Zhang SD, Liang JZ, Wang JZ (2015) Effect of polyethylene glycol on the crystallization and impact properties of polylactide-based blends. Polym Adv Technol 26:465–475
16. Diaz CA, Pao HY, Kim S (2016) Film performance of poly(lactic acid) blends for packaging applications. J Appl Packag Res 8:42–51
17. Ferri JM, Fenollar O, Jorda-Vilaplana A, García-Sanoguera D, Balart R (2016) Effect of miscibility on mechanical and thermal properties of poly(lactic acid)/polycaprolactone blends. Polym Int 65:453–463
18. Pattamaprom C, Chareonsalung W, Teerawattananon C, Ausopron S, Prachayawasin P, Van Puyvelde P (2016) Improvement in impact resistance of polylactic acid by masticated and compatibilized natural rubber. Iran Polym J 25:169–178
19. Semba T, Kitagawa K, Ishiaku US, Hamada H (2006) The effect of crosslinking on the mechanical properties of polylactic acid/polycaprolactone blends. J Appl Polym Sci 101:1816–1825
20. Bach C, Dauchy X, Severin I, Munoz J-F, Etienne S, Chagnon M-C (2013) Effect of temperature on the release of intentionally and non-intentionally added substances from polyethylene terephthalate (PET) bottles into water: chemical analysis and potential toxicity. Food Chem 139:672–680
21. Zemljič LF, Tkavc T, Vesel A, Šauperl O (2013) Chitosan coatings onto polyethylene terephthalate for the development of potential active packaging material. Appl Surf Sci 265:697–703
22. Inuwa I, Hassan A, Wang D-Y, Samsudin S, Haafiz MM, Wong S, Jawaid M (2014) Influence of exfoliated graphite nanoplatelets on the flammability and thermal properties of polyethylene terephthalate/polypropylene nanocomposites. Polym Degrad Stabil 110:137–148
23. Xia X-L, Liu W-T, Tang X-Y, Shi X-Y, Wang L-N, He S-Q, Zhu C-S (2014) Degradation behaviors, thermostability and mechanical properties of poly(ethylene terephthalate)/polylactic acid blends. J Central South Univ 21:1725–1732
24. Chen H, Pyda M, Cebe P (2009) Non-isothermal crystallization of PET/PLA blends. Thermochim Acta 492:61–66
25. Torres-Huerta AM, Palma-Ramírez D, Dominguez-Crespo MA, Del Angel-López D, De La Fuente D (2014) Comparative assessment of miscibility and degradability on PET/PLA and PET/chitosan blends. Eur Polym J 61:285–299
26. Nam B-K, Park OO, Kim S-C (2015) Properties of isotactic polypropylene/atactic polypropylene blends. Macromol Res 23:809–813
27. Saeidlou S, Huneault MA, Li H, Park CB (2012) Poly(lactic acid) crystallization. Prog Polym Sci 37:1657–1677
28. Cardinaud R, McNally T (2013) Localization of MWCNTs in PET/LDPE blends. Eur Polym J 49:1287–1297

29. Yang JH, Shen Y, He WD, Zhang N, Huang T, Zhang JH, Wang Y (2013) Synergistic effect of poly(ethylene glycol) and graphene oxides on the crystallization behavior of poly(l-lactide). J Appl Polym Sci 130:3498–3508

30. Lasprilla AJ, Martinez GA, Lunelli BH, Jardini AL, Maciel Filho R (2012) Poly-lactic acid synthesis for application in biomedical devices—a review. Biotechnol Adv 30:321–328

31. Raquez J-M, Habibi Y, Murariu M, Dubois P (2013) Polylactide (PLA)-based nanocomposites. Prog Polym Sci 38:1504–1542

32. Zhao Y, Lang X, Pan H, Wang Y, Yang H, Zhang H, Zhang H, Dong L (2015) Effect of mixing poly(lactic acid) with glycidyl methacrylate grafted poly(ethylene octene) on optical and mechanical properties of the blown films. Polym Eng Sci 55:2801–2813

33. Patcheak TD, Jabarin SA (2001) Structure and morphology of PET/PEN blends. Polymer 42:8975–8985

34. Chen D, Gao X, Dollimore D (1993) A generalized form of the Kissinger equation. Thermochim Acta 215:109–117

35. Jabarin S (1987) Crystallization kinetics of polyethylene terephthalate. II. Dynamic crystallization of PET. J Appl Polym Sci 34:97–102

36. Xue M-L, Sheng J, Yu Y-L, Chuah HH (2004) Nonisothermal crystallization kinetics and spherulite morphology of poly(trimethylene terephthalate). Eur Polym J 40:811–818

37. Ziabicki A (1974) Theoretical analysis of oriented and non isothermal crystallization. Colloid Polym Sci 252:207–221

38. Sajkiewicz P, Carpaneto L, Wasiak A (2001) Application of the Ozawa model to non-isothermal crystallization of poly(ethylene terephthalate). Polymer 42:5365–5370

39. Di Lorenzo M, Silvestre C (1999) Non-isothermal crystallization of polymers. Prog Polym Sci 24:917–950

40. Lu X, Hay J (2001) Isothermal crystallization kinetics and melting behaviour of poly(ethylene terephthalate). Polymer 42:9423–9431

41. Li W, Kong X, Zhou E, Ma D (2005) Isothermal crystallization kinetics of poly(ethylene terephthalate)–poly(ethylene oxide) segmented copolymer with two crystallizing blocks. Polymer 46:11655–11663

42. Hafsia KB, Ponçot M, Chapron D, Royaud I, Dahoun A, Bourson P (2016) A novel approach to study the isothermal and non-isothermal crystallization kinetics of poly(ethylene terephthalate) by Raman spectroscopy. J Polym Res 23:93